The 7th International Supercritical CO_2 Power Cycles Symposium
February 21 – February 24, 2022, San Antonio, Texas
Paper # 121

Integrated Transient Modeling of Gas Turbine and sCO_2 Power Cycle for Exhaust Heat Recovery Application

Vamshi K. Avadhanula
Systems Engineer
Echogen Power Systems (DE), Inc.
vavadhanula@echogen.com

Timothy J. Held
Chief Technology Officer
Echogen Power Systems (DE), Inc.
theld@echogen.com

Abstract

For distributed generation installations, the transient response of the power generation system is critical to meet power quality (voltage and frequency) requirements. Transient models for gas turbine and supercritical carbon dioxide (sCO_2) power cycle were integrated for an exhaust heat recovery bottoming cycle system for a distributed generation application. The transient model for the SGT-750 Siemens gas turbine was a 'black-box' functional mockup interface (FMI) model developed by Siemens Industrial Turbomachinery in Finspång, Sweden. The SGT-750 is a twin-shaft gas turbine that produces 40 MW electricity with an efficiency of about 40% at ISO conditions. At 100% gas turbine throttle (load), the SGT-750 has average exhaust conditions of 114.6 kg/s and 469.8°C.

The transient model for sCO_2 power cycle was developed by Echogen in GT-SUITE 1D system simulation software platform. The basic CO_2 flow circuit has single-shaft turbomachinery with net 11.5 MW electrical power output at design conditions. The power turbine has a double-ended shaft with one end connected to synchronous generator through a fixed-ratio gearbox. The other end of power turbine is connected to the compressor through a continuously variable transmission. The major components of the sCO_2 power cycle modeled include air cooled condenser/cooler, CO_2 compressor, recuperator, two waste heat exchanger coils, power turbine, continuous variable transmission, gearbox and generator. Apart from the component models, the sCO_2 power cycle model also includes the control system modeling for smooth operation of the cycle as grid load demand changes.

In the integrated model, the gas turbine and sCO_2 power cycle interact at two points, first one being the gas turbine exhaust gas flow rate and temperature, which are inputs to sCO_2 power cycle model. The second point is the distribution of grid load demand signal between the SGT-750 generator and sCO_2 cycle generator. For a given combined-cycle load demand, the gas turbine load demand is equal to the total demand minus the sCO_2 cycle power generated. For the transient simulations, a representative 5 MWe step load demand profile is used as input. Finally, the time series plots representing load step versus integrated system response are presented including the sCO_2 power cycle control system performance plots.

Nomenclature

WHX1 and WHX2 waste heat exchanger coil-1 and coil-2
RHX1 recuperative heat exchanger
ACC air cooled condenser/cooler
CVT continuous variable transmission
PT power turbine

FMI Functional mock-up interface
FMU Functional mock-up unit
MCSF minimum continuous stable flow
TEOC Matlab Techno-Economic Optimization Code
EPS100 Echogen's 7.3 MW commercially available sCO_2 Brayton power system
ICS CO_2 inventory control system
w_c PT corrected mass flow rate
w PT actual mass flow rate
η_s PT isentropic efficiency
N_c PT corrected speed
N PT actual speed
dh_{sc} PT corrected isentropic enthalpy drop
dh_s PT actual isentropic enthalpy drop
Z CO_2 compressibility factor
γ Ratio of specific heats
T Temperature in K
p Pressure in MPa
GB_{loss} Gearbox losses
Brg_{loss} PT Bearing losses
Gen_{loss} Generator losses
PT_{kW} Power turbine total kW

1 Intoduction

In recent years Supercritical carbon dioxide (sCO_2) power cycles have gained lot of attention due its advantages over conventional steam Rankine cycle, such as higher efficiency, lower capital and operating costs, smaller physical footprint and water-free operation [1, 2, 3]. sCO_2 power cycles are being studied in the areas of advanced nuclear cycles [4, 5, 6], concentrated solar power (CSP) systems [7, 8, 9], waste and exhaust heat recovery [1, 10, 11], and oxyfuel combustion cycles for primary power [12]. sCO_2 power cycles were first considered as gas turbine bottoming cycles in late 1970's for its use in shipboard applications [13]. Many of these studies have primarily focused on theoretical cycle development, although significant advances have been made in laboratory-scale experimental systems [14, 6]. In the industrial scale category, Echogen has tested a nominal 7.3 MWe net power sCO_2 power cycle designed for commercial operation, utilizing the exhaust heat from a 20-25 MWe gas turbine as the heat source [15, 16]. More recently Department of Energy has partially funded to design, construct, and operate 10 MWe sCO_2 pilot plant test facilities, under STEP (Supercritical Transformational Electric Power) program [17, 18]. Echogen Power Systems has recently completed a FEED study for 10 MWe sCO_2 pilot plant under Large Scale Pilot program again partially funded by DOE [19].

In the present study transient models for gas turbine and supercritical carbon dioxide (sCO_2) power cycle were integrated for an exhaust heat recovery bottoming cycle system for a distributed generation application. For the integrated transient model the input boundary conditions are grid load demand and ambient conditions.

The transient model for the SGT-750 Siemens gas turbine was a "black-box" functional mock-up interface (FMI) [20] model developed by Siemens Industrial Turbomachinery in Finspång , Sweden. The SGT-750 is a twin-shaft gas turbine that produces 40 MW electricity with an efficiency of about 40% at ISO conditions. At 100% gas turbine throttle (load), the SGT-750 has average exhaust conditions of 114.6 kg/s and 469.8 °C. Section "Transient Models Assembled" below gives more discussion on the integration of SGT-750 transient model and sCO_2 power cycle transient model.

Figure 1 shows the sCO_2 power cycle architecture considered for this study. The basic CO_2 flow circuit has single-shaft turbomachinery. The power turbine (PT) has double ended shaft with one end connected to synchronous generator through constant ratio gearbox. The other end of PT connected to compressor through continuous variable transmission (CVT). CVT is used to maintain compressor outlet pressure by varying gear ratio which in turn correspond to a compressor speed. Compressor pressurizes CO_2 from the air-cooled heat exchanger (ACC), state-1 in figure 1, to supercritical pressures (state-2). This high-pressure CO_2 is split between waste heat exchanger coil-2 (WHX2) (state-21) and the recuperator (RHX1) (state-22). The high-pressure CO_2 exchanges heat with turbine exit flow (state-5) in high temperature recuperator (RHX1). This relatively high-enthalpy CO_2 flow (state-32) mixes with flow from WHX2 (state-31). This mixed flow (state-3) exchanges heat in WHX coil-1 (WHX1) with gas turbine exhaust. This high-enthalpy CO_2 (state-4) is expanded in power turbine (PT) which in turn rotates a generator connected through a speed-reducing gearbox on one end and CVT-compressor on another end. The turbine exit flow (state-5) (low pressure – high temperature fluid) exchanges heat with high pressure CO_2 from the compressor in RHX1 before condensing or cooling in ACC, and the cycle continues. Note that figure 1 and the state points shown will be actively used in the present study for reference.

In sCO_2 power cycle operation, the compressor inlet pressure (system low pressure, state-1) is controlled using an active inventory control system, while compressor outlet pressure (system high pressure, state-2) is controlled by varying compressor speed using CVT. Compressor outlet flow is split between WHX2 and RHX1 using a flow split valve at WHX2 inlet to maintain equal sCO_2 outlet temperature (T31=T32) for both heat exchangers. sCO_2 cycle generator load is controlled to maintain synchronous generator speed at 60 Hz.

The transient model for sCO_2 power cycle was developed by Echogen in GT-SUITE [21] 1D system simulation software platform. In flow simulations (of present work), GT-SUITE solves 1D Navier-Stokes equations along flow components and solution convergence is checked using pressure, continuity and energy residuals. The models are built based on GT-SUITE supplied and/or user-defined component templates. Component templates can take manufacturer data and/or test data to size the component. Individual components can then be simulated using subsystem boundary conditions before being incorporated into full system model. These component templates are connected by piping components to build the full system model. GT-SUITE uses NIST REFPROP [22] for fluid thermal and transport properties. Echogen has previously verified the GT-Suite transient model results against the test data from its commercially-available nominal 7.3 MWe (the EPS100) net power sCO_2 power cycle [15, 16].

The following sections and subsections describe in detail the sCO_2 power cycle components considered in developing the full system transient model, the control system parameters for sCO_2 cycle smooth operation and the steps taken in integrating the gas turbine and sCO_2 power cycle transient models. For the transient simulations, a 5 MWe step load demand profile was used as input. Finally, in the "Results and Discussion" section the time series plots representing step load demand versus integrated system response are presented including the sCO_2 power cycle control system performance plots. Note that for all the modeling and simulations of present study ambient temperature is fixed at 15 °C.

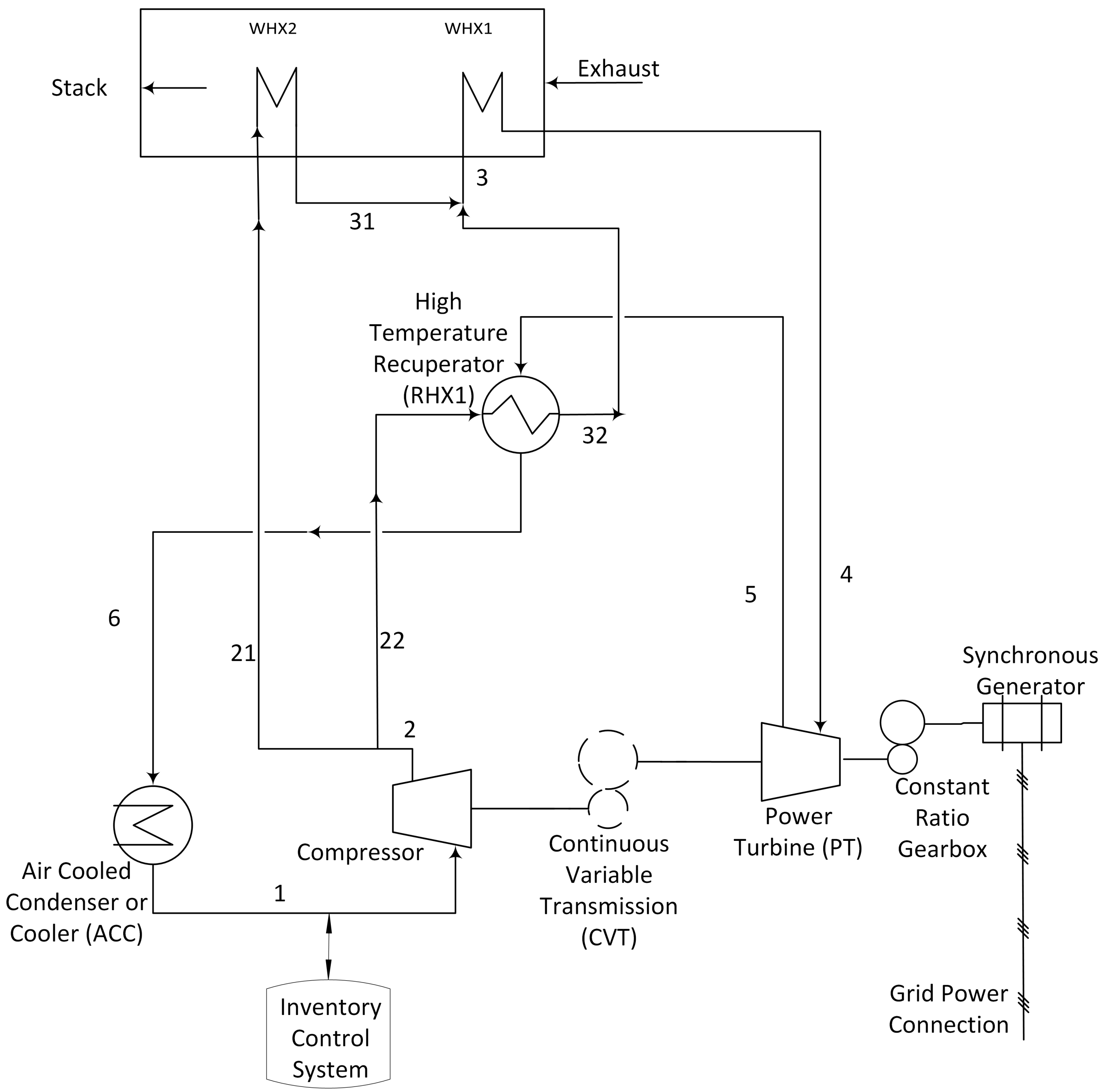

Figure 1: Schematic of sCO_2 power cycle architecture considered

2 sCO_2 and Gas Turbine Transient Models Development

The following sections discuss the sCO_2 and gas turbine transient models development which will be used later for combined (or integrated) cycle simulations. SGT-750 Siemens gas turbine transient model provided by Siemens Finspång is discussed briefly. sCO_2 power cycle transient model development in GT-Suite is discussed in detail which includes cycle design point selection process, cycle individual component selection for transient runs, sCO_2 cycle control system and lastly the modeled sCO_2 cycle in GT-Suite.

2.1 Gas Turbine Transient Model Development

Siemens Finspång has provided Echogen with SGT-750 Siemens gas turbine model for the first integration study with the sCO_2 power cycle model as a exhaust heat recovery bottoming cycle. The SGT-750 gas turbine transient model is a “black-box” functional mock-up unit (FMU) [20] which can be integrated with the sCO_2 power cycle model developed in GT-SUITE using Matlab/Simulink as the integration tool. SGT-750 is twin shaft gas turbine which produces 40 MW electricity with an efficiency of about 40% at ISO conditions. At 100% gas turbine throttle (load), the SGT-750 has average exhaust conditions at 114.6 kg/s and 469.8 °C. Section “Transient Models Assembled” below gives more discussion on the integration of SGT-750 transient model and sCO_2 power cycle transient model using representative step load demand.

2.2 sCO_2 Power Cycle Transient Model Development

The transient model for sCO_2 power cycle was developed by Echogen in GT-SUITE [21] 1D system simulation software platform. In the present study, the transient sCO_2 power cycle simulations involve two parts: first, steady-state cycle optimization runs throughout the ambient temperature range to select the basis design and its equipment sizes (heat exchangers, turbomachinery, valves etc.) for building an sCO_2 cycle transient model; second, transient model development of the power cycle itself based on the steady state optimization simulation results. Transient simulation results will be compared with the steady state optimization results for model validation.

In sCO_2 power cycle operation, the compressor inlet pressure (system low pressure, state-1) is controlled using an active inventory control system, while compressor outlet pressure (system high pressure, state-2) is controlled by varying compressor speed using CVT. Compressor outlet flow is split between WHX2 and RHX1 using a flow split valve at WHX2 inlet to maintain equal sCO_2 outlet temperature (T31=T32) for both heat exchangers. sCO_2 cycle generator load is controlled to maintain synchronous generator speed at 60 Hz.

2.2.1 Steady State Optimization Model

To establish the baseline sCO_2 power cycle net output and its equipment sizes (heat exchangers, turbomachinery, valves etc.) for building an sCO_2 transient model, Echogen’s TEOC was used in a three-step process. At the end of this process, the TEOC outputs (referred to as “Optimizer Results”) will include sCO_2 power cycle steady state performance predictions, along with equipment sizes and preliminary power turbine maps to be used later in transient modeling. Table 1 gives the boundary condition and constraints considered for designing the sCO_2 architecture (figure 1) of present study. The boundary conditions correspond to ISO conditions of SGT-750 gas turbine. As noted above, ambient temperature is fixed at 15 °C. Maximum allowable power cycle pressure of 25 MPa, minimum allowable power cycle temperature at 5 °C and minimum allowable exhaust gas stack outlet temperature at 85 °C values were based on project team’s previous experience.

Table 1: sCO_2 cycle boundary condition and constraints considered for design as well as selected cycle equipment performance at design point (both TEOC and transient model simulation results)

sCO_2 cycle design point boundary conditions				**sCO_2 cycle constraints**		
Exhaust flow (kg/s)	Exhaust temperature (°C)	Ambient temperature (°C)		Minimum exhaust stack temperature (°C)	Maximum sCO_2 cycle pressure (MPa)	Minimum allowable power cycle temperature (°C)
114.6	469.8	15.00		85.00	25.00	5
Cycle Modeling Results						
State Point in figure 1	**Steady state model results**			**GT-Suite transient model results compared to steady state results**		
	Flow (kg/s)	T (°C)	P (MPa)	Flow (kg/s)	T (°C)	P (MPa)
1	152.38	23.80	6.94	151.49	23.43	6.97
2	152.38	48.57	25.00	151.49	48.50	24.97
21	56.10	48.49	24.82	56.94	48.42	24.76
22	96.28	48.57	25.00	94.55	48.51	24.97
31	56.10	254.50	24.62	56.94	255.63	24.58
32	96.28	253.41	24.62	94.55	255.68	24.62
3	152.38	253.81	24.62	151.49	255.61	24.57
4	152.38	379.76	24.32	151.49	381.94	24.19
5	152.38	260.07	7.24	151.49	261.21	7.12
6	152.38	63.16	7.14	151.49	65.42	7.02
Exhaust stack temperature		107.18			106.47	
WHX1 heat transfer rate (kW)	24590.07			24504.73		
WHX2 heat transfer rate (kW)	20704.37			21114.05		
RHX1 heat transfer rate (kW)	35392.51			35057.12		
ACC heat transfer rate (kW)	32107.56			32933.88		
Power (kW)	16804.68			16920.87		
Compressor (kW)	4085.26			4235.98		
ACC fan load (kW)	466.12			502.48		
Auxiliary losses (gearbox, generator and CVT) (kW)	743.74			685.60		
Generator (kW)	11509.56			11496.80		
Cycle efficiency (%)	25.41			25.20		

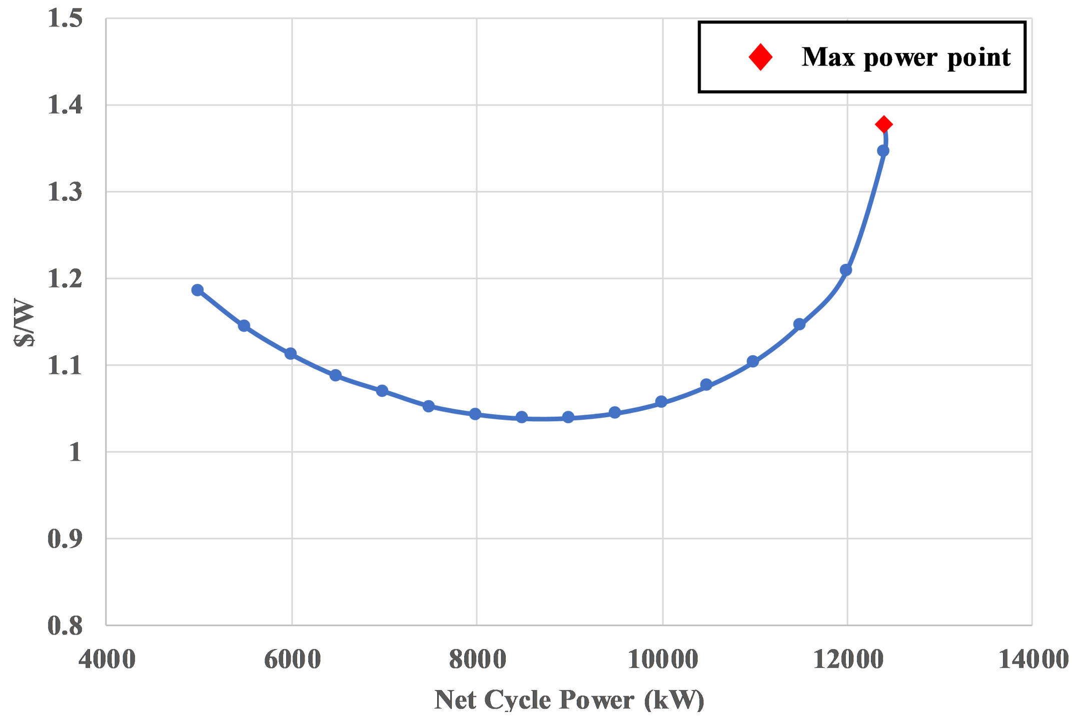

Figure 2: Cost per watt versus net cycle power for 15 °C ambient temperature

The first step involves determining the maximum power that can be generated for the sCO_2 architecture and design conditions (table 1) considered. For obtaining this point, the TEOC is run for 'power optimization' with no constraints on equipment sizes. As shown in figure 2 (marked with 'red diamond'), the sCO_2 cycle has maximum net power output of about 12.4 MW. The second step involves determining the equipment sizes—basically, heat exchanger conductance (UA) and turbomachinery maps—using the TEOC for cost optimization. Basically, the TEOC is run for 'cost optimization' by incrementally decreasing the target net cycle power output starting from maximum power value to obtain a curve for system cost ($/W) versus net cycle power (kW) as shown in figure 2. Based on these results, the 11.5 MW case, which has $1.15/W for sCO_2 power cycle equipment, was selected as baseline for this study.

The third and final step in optimization involves determining the cycle performance prediction for ambient range of −25 °C to 40 °C by fixing heat exchanger sizes (UAs) and turbomachinery maps from the 11.5 MW case selected in step two above. Figure 3 gives net cycle power output from this optimizer run. Table 1 gives the detailed TEOC performance prediction results for the design case of 15 °C ambient under the column "Steady state model results". The results from this optimizer run are used in transient modeling for sizing the heat exchangers and validating the transient model results for steady state operation. Further results from these optimizer runs are included in later section component sizing and transient model validation.

2.2.2 Component Selection for Transient Model

Considering the above steady state result as design point for sCO_2 cycle, heat exchangers and compressor components were selected for transient modeling from manufacturer's quotations or catalogs. In the current sCO_2 cycle under consideration, four heat exchangers have been modeled: WHX1, WHX2, RHX1 and ACC. In modeling of heat exchangers in GT-SUITE, the heat transfer

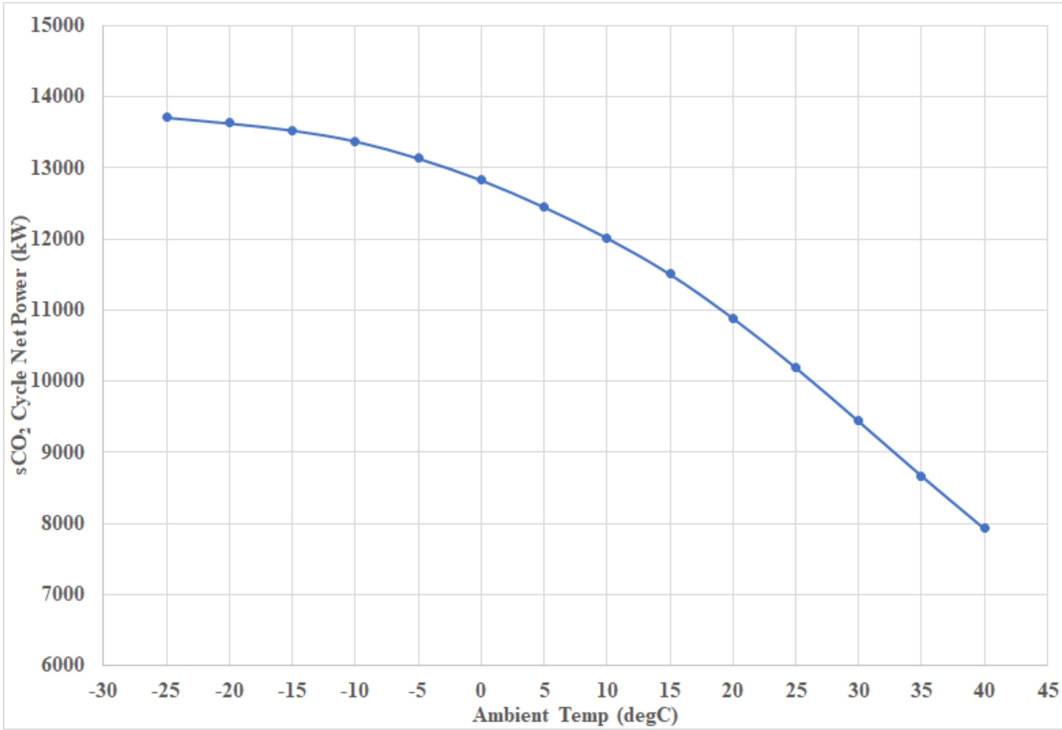

Figure 3: Net cycle power versus ambient temperature for the selected sCO_2 cycle components

process is discretized into 25 sub-volumes to account for the variation in fluid properties as the temperature and pressure vary across the length of the heat exchanger. The thermal mass of the heat exchanger is set equal to the physical dry mass of the heat exchanger multiplied by the average heat capacity of the 316L stainless steel material. Heat exchangers similar to those in the present study were modeled in GT-Suite by project authors and have been previously published [23]. All the heat exchangers used in transient modeling were selected from previous manufacturer quotations of similar sizes predicted by optimization code (table 1).

The compressor was selected from a pump manufacturer's catalog based on design point, and the corresponding pump curve was used in transient simulations. For the sCO_2 power turbine, in-house available Concepts NREC turbomachinery meanline software code was used to create a preliminary design for a two-stage axial turbine and generate the performance map for the present study's transient model.

Waste Heat Exchanger: In the gas turbine exhaust heat recovery of present study, within the waste heat exchanger coils (WHX1 and WHX2), exhaust gases on the fin side transfer heat to high-pressure CO_2 (from compressor and recuperator) on the tube side. For the finned-tube waste heat exchanger coils, GT-SUITE's built-in finned-tube heat exchanger model templates were used for simulations. Physical geometry information was taken from a manufacturer-provided quotation of similar size heat exchangers and is given in table 2. The WHX coils were modeled as single-phase heat transfer with CO_2 on tube side and gas turbine exhaust as fin side fluids. For heat transfer coefficients, on CO_2 side classical Dittus-Boelter corrections were used and Colburn correlation on exhaust side, with one-dimensional thermal conduction resistance between the two fluids. Standard friction factor correlations were used to model pressure loss coefficients on both tube and fin sides.

Recuperator: Within the recuperator, relatively low-pressure, high-temperature CO_2 from the turbine exhaust transfers heat to the high-pressure, low-temperature CO_2 from the compressor

Table 2: WHX1, WHX2 and ACC physical parameters

	WHX1	WHX2	ACC: single-bay
Dry mass, kg	92,532.8	174,179	20,030.6
Height(m) x Width(m) x Depth(m)	11 x 6.5 x 3.6	11 x 6.5 x 3.6	4.3 x 15.8 x 0.33
Inlet connection diameter, cm (in)	28.4 (11.2)	17.3 (6.8)	29.2 (11.5)
Outlet connection diameter, cm (in)	32.5 (12.8)	17.3 (6.8)	29.2 (11.5)
Circular channel diameter, cm (in)	3.81 (1.5)	3.81 (1.5)	2.2 (0.87)
Fin density, 1/m (1/in)	236 (6)	236 (6)	394 (10)
Number of tubes in the direction of exhaust (or air) flow	5	10	6
Number of tubes perpendicular to the direction of exhaust (or air) flow	64	64	67
Total number of bays	-	-	6
Fans per bay (total fans)	-	-	3 (18)

discharge. In an installed system recuperator (RHX1) would be a printed circuit heat exchanger (PCHE) [24], but for the present study it is simulated as a plate heat exchanger (PHE) in GT-Suite (using built-in template) with increased heat transfer area multiplier to account for the higher effectiveness of the PCHE geometry. From a heat transfer and pressure loss perspective, PCHEs and PHEs have very similar governing equations, as both are primarily counterflow geometry, and the fluid flow is well within the turbulent regime. Thus, the PCHE can be simulated by applying an increased heat transfer area multiplier to account for the smaller passage dimensions relative to a conventional PHE. Table 3 gives the physical parameters considered in modeling RHX1. A value of six (6) for heat transfer area multiplier was from previous experience [16, 23] of the authors in modeling similar heat exchangers in GT-Suite. Single-phase heat transfer was considered on both fluid sides of the recuperator and again heat transfer coefficients are based on single-phase Dittus-Boelter correlations on both fluid sides, with one-dimensional thermal conduction resistance between the two fluids.

Air Cooled Condenser/Cooler: In ACC CO_2 on the tube side (from low pressure side of recuperator outlet) transfers heat to the cross-flowing cooling air from ACC fans on the fin side. ACC is a finned-tube heat exchanger with three fans per bay. GT-SUITE's built-in finned-tube heat exchanger model templates were used for simulations. Physical geometry information was taken from a manufacturer-provided quotation and is given in table 2 for single-bay. A total of six bays (6) were used in the present model. The CO_2 flow from RHX1 outlet is distributed almost uniformly among six bays and the cooled (or condensed) CO_2 from each bay is converged into a single header before returning to the compressor inlet. Modeling of the ACC involves two components, heat exchanger model (tube bundle) as well as fan model using fan curves from manufacturer. The ACC was modeled as two-phase heat transfer on tube side and single-phase on fin side as it is designed

Table 3: RHX1 physical parameters

Dry mass, kg	10,400
Plate length (cm)	156.2
Plate width (cm)	59.6
Plate wall thickness (mm)	4
High pressure side connection diameter, cm (in)	21.6 (8.5)
Low pressure connection diameter, cm (in)	54.7 (21.5)
Number of plates of high and low pressure side	300
Heat transfer area multiplier	6

to operate in both supercritical and transcritical (condensing) mode. On tube side, for single-phase heat transfer, Dittus-Boelter correlations are used, while the correlation of Dobson and Chato [25] was used for condensation heat transfer. Also on CO_2 side, for single phase, standard friction factor correlations and for two-phase Friedel [26] correlations were used to model pressure loss coefficients in tubes. For air side, Colburn correlation for heat transfer coefficients and standard friction factor correlation were used to model pressure loss coefficients.

The sizing process was validated by using a subcomponent model, which includes the heat exchanger and inlet conditions. The GT-SUITE modeled outlet temperatures are shown in figure 4 (for WHX1 and WHX2), figure 5 (for RHX1) and figure 6 (for ACC) as a function of optimizer outlet temperatures on both fluid sides, and the agreement is excellent.

Compressor: State-1 and state-2 data in table 1 was used as design point conditions for selecting a compressor/pump curve from Sulzer pump catalog [27]. Figure 7 shows the compressor/pump curve selected from Sulzer catalog with design point data shown, at which compressor has flow, pressure rise and efficiency of $722\,\mathrm{m^3\,h^{-1}}$, 18.06 MPa and 75 % respectively. Compressor curve was directly supplied to the compressor/pump template in GT-Suite for transient simulations.

Power Turbine Conceptual Design and Map Development: The sCO_2 power turbine conceptual design and performance map development was done in-house by Echogen using commercially available turbomachinery meanline code from Concepts NREC. State-4 and state-5 data in table 1 was used as design point. Two-stage axial turbine was considered for this application with the design constraints given in table 4. A parametric study was done varying meanline code's internal non-dimensional factors (such as coefficients of axial size, area, reaction, clearance etc.) until a axial design satisfying all the constraints was obtained. Table 4 also gives the achieved constraint values for the selected design. Once the axial turbine design is selected, the physical parameters of the turbine (e.g. number of blades, hub diameter, hub-to-tip ratios etc.) are fixed for further turbine analysis and map generation.

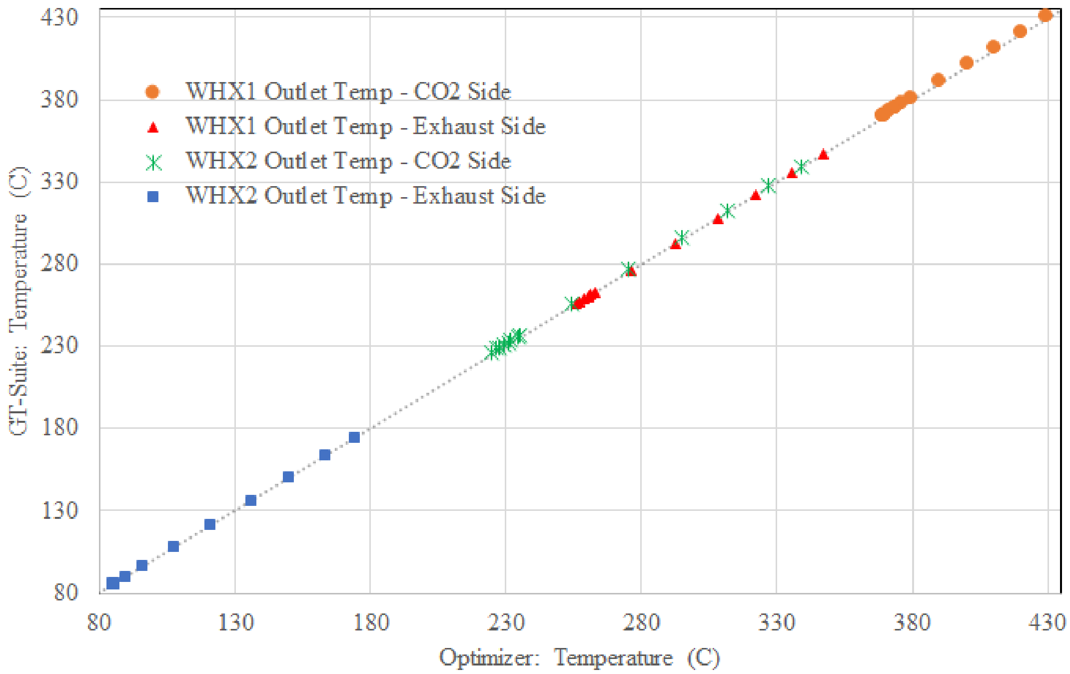

Figure 4: WHX1 and WHX2 outlet temperatures for individual component model calibration in GT-Suite

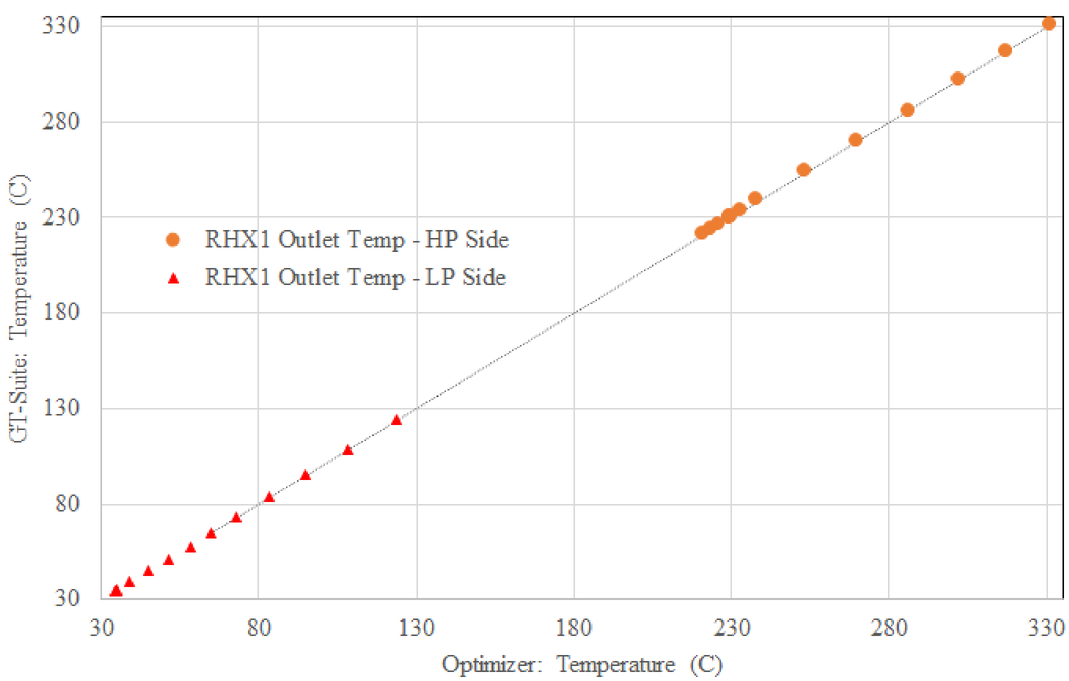

Figure 5: RHX1 outlet temperatures for individual component model calibration in GT-Suite.

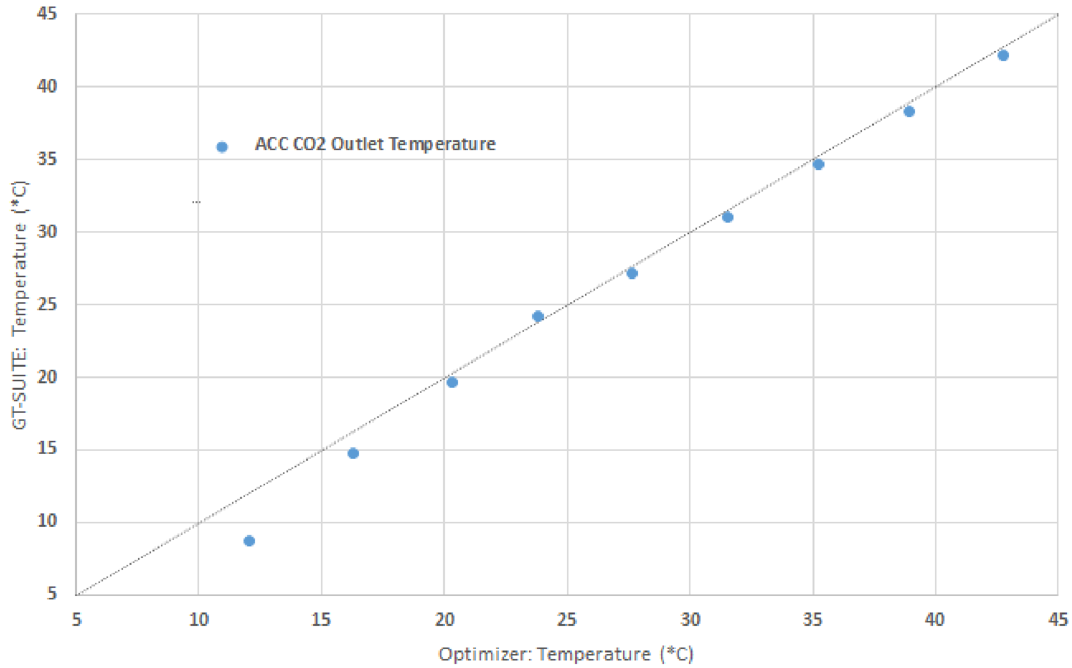

Figure 6: ACC outlet temperatures for individual component model sizing in GT-Suite.

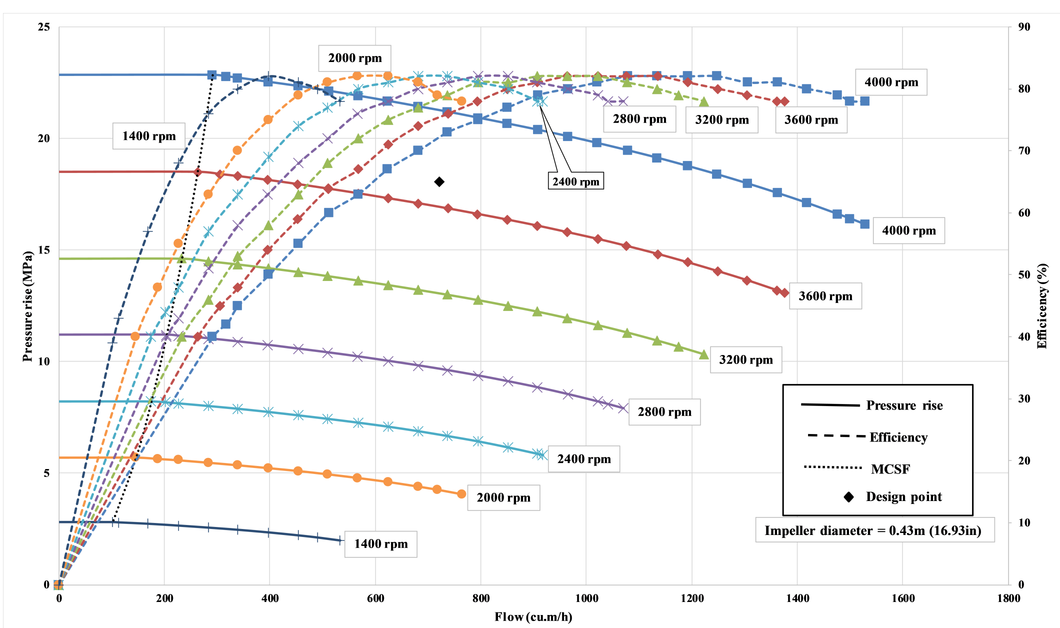

Figure 7: Compressor curve used in transient simulations of sCO_2 cycle

Table 4: Two-stage axial turbine design constraints considered and achieved values

	Design Constraint		**Design Achieved Values**
Parameter	**Min**	**Max**	
Shaft Power (kW)	17000	-	17326.2
Stress (MPa)	-	360	132.679
(AN)^2 (m^2*rpm^2)	-	2.80E+07	6.20E+06
Zweifel factor in Rotors	-	1.15	0.645735
Zweifel factor in Stators	-	1.15	0.655249
Seal tip clearance (mm)	0.1	1	0.3
Blade height (m)	0.007	-	0.0128691
Hub separation between blades (m)	0.0025	-	0.0103891
Pressure reaction in rotors (ReactionPts)	0.05	0.6	0.537491
Hub speed (m/s)	-	320	231.055

For the selected design of two-stage axial turbine some of the other parameters from the meanline code are: turbine efficiency=86.2%, speed=15000rpm, pressure ratio=3.6, number of blades for stage-1 stator, stage-1 rotor, stage-2 stator and stage-2 rotor are 34, 33, 33, and 30 respectively.

Once the meanline design of the turbine is fixed, the next step involves generation of turbine map over an expected operating range. For the present study axial turbine map was generated by varying three parameters over the following ranges: Speed:5000 rpm to 25000 rpm increments of 1000 rpm; pressure ratio: 1.5 to 7.0 increments of 0.5; and turbine inlet temperature 287.9 °C to 429.7 °C (based on gas turbine performance). Figure 8 and figure 9 shows the generated map for a turbine inlet temperature and pressure of 379.76 °C and 24.32 MPa respectively.

GT-Suite has the ability to input the raw turbine map generated using meanline code. The generated power turbine map in meanline code was directly supplied to GT-Suite turbine template for parameters of speed, mass flow rate, turbine inlet pressure, temperature and outlet pressure, efficiency and shaft power. For any intermediate points GT-Suite performs linear interpolation based on speed, inlet pressure, inlet temperature, outlet temperature to predict the turbine performance i.e. mass flow rate, efficiency, power etc.

Powertrain Mechanical Losses: The mechanical model of the turbomachinery, gearbox and generator uses the classical rotational inertia formulation to create the angular momentum conservation equation for the transient simulation. Mechanical losses are modeled from previous experimental data from EPS100 for the turbine bearings, gearbox and generator. The bearing and gearbox losses are functions of power turbine speed, and generator loss is function of power turbine speed and power turbine load. CVT efficiency of 97% was considered for present sCO_2 cycle study.

$$GB_{loss} = f(N)$$
$$Brg_{loss} = f(N)$$
$$Gen_{loss} = f(N, PT_{kW})$$

2.2.3 sCO_2 Cycle Control System Models

The control loops follow a basic proportional-integral configuration, with a measured parameter used as the feedback variable to drive the behavior of a control variable. An example is shown in

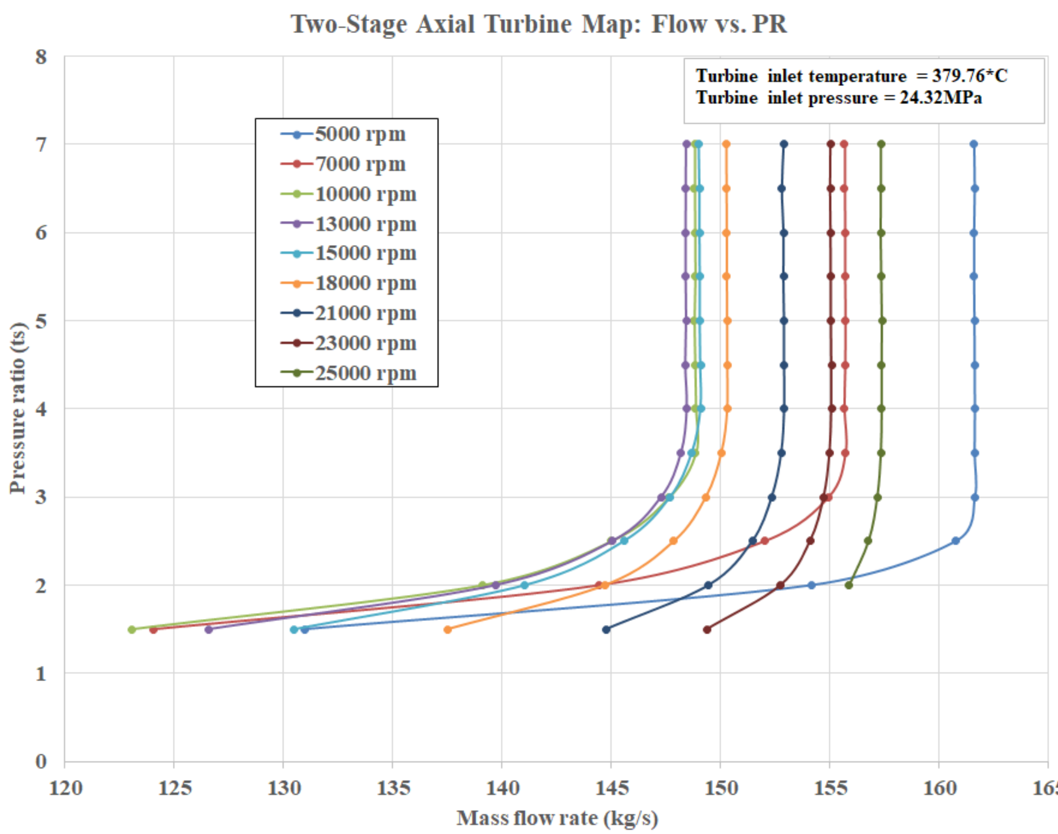

Figure 8: Two-stage axial turbine map (flow vs. PR) used in transient simulations of sCO_2 cycle

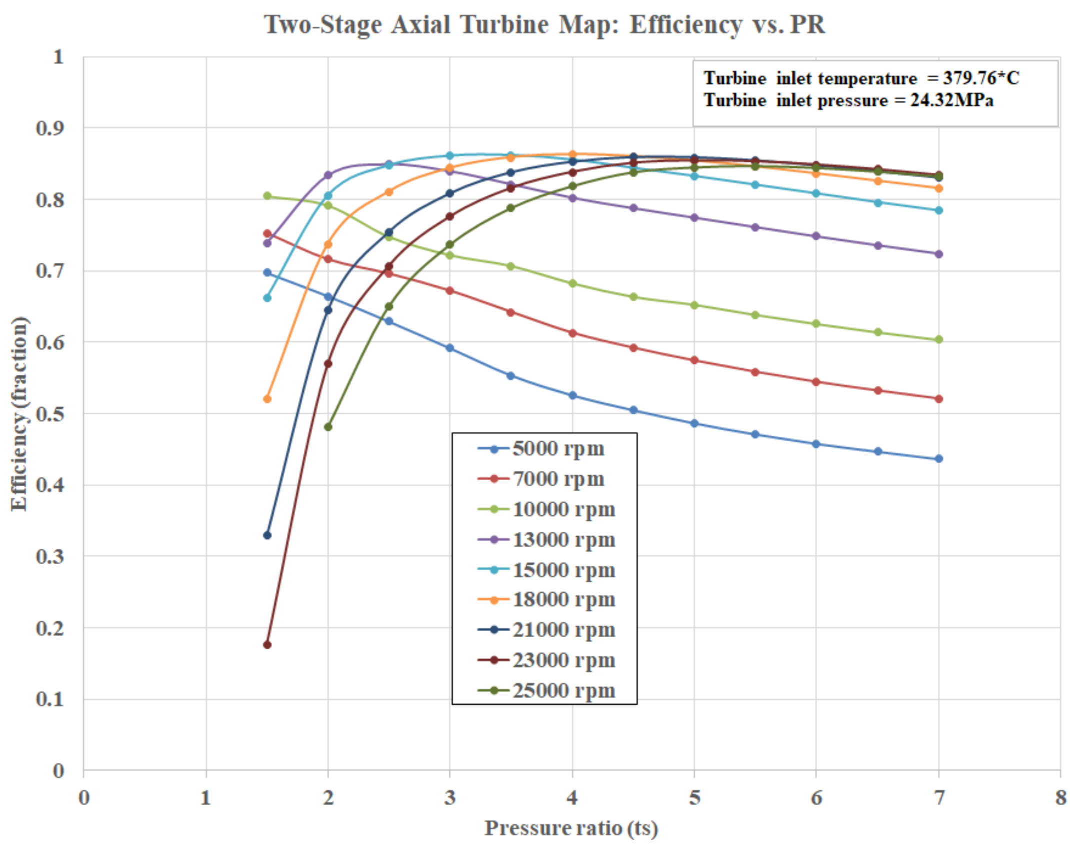

Figure 9: Two-stage axial turbine map (Efficiency vs. PR) used in transient simulations of sCO_2 cycle

Figure 10, which depicts the compressor outlet pressure control loop. The measured compressor outlet pressure is compared to the pressure setpoint. The difference between the measured and setpoint pressure is used to modify the continuous variable transmission (CVT) gear ratio, using classical proportional-integral (PI) formulations, with the proportional gain and integral times defined by the operator. Much of the process of ”tuning” a control system consists of modifying these parameters to obtain optimal response time of the system to disturbances while maintaining fully stable operation.

In the present sCO_2 power cycle transient model four major control parameters have been modeled which include:

- Compressor inlet pressure (designated as P1) using inventory control system (ICS). ICS is modeled and the respective components are shown in Figure 11. ICS maintains the compressor inlet pressure to a setpoint pressure by adding or removing CO_2 from/to a storage tank. The setpoint pressure is determined by ACC CO_2 outlet temperature which in turn depends on ambient temperature. ICS maintains compressor inlet pressure roughly around 100 psi above saturation pressure which is determined at ACC CO_2 outlet temperature.
- Continuous variable transmission (CVT) maintains compressor outlet pressure (designated as P2) at a setpoint while maintaining exhaust stack temperature above 85 °C. Both P2 and exhaust stack temperature are given as function of exhaust temperature and exhaust pressure drop in WHX coils. A 2D table, generated using optimizer (TEOC) data, is supplied to the model which determines the P2 setpoint and the CVT gear ratio is modified to maintain P2 at setpoint while checking exhaust stack temperature.

$$P2 = f(T_{exht}, dP_{exht})$$

- Generator speed is controlled to synchronous speed of 1800 rpm by varying generator load
- CO_2 flow to WHX2 coil is varied by controlling lift on a flow split valve to match WHX2 and RHX1 outlet temperatures

2.2.4 sCO_2 Power Cycle Model in GT-Suite

Figure 11 shows, on GT-SUITE platform, the sCO_2 power cycle model configuration with air cooled condenser/cooler (ACC), compressor, recuperator (RHX1), waste heat exchanger coils (WHX1 and WHX2), power turbine, CVT, gearbox and generator including control system components. Individual component models were first constructed and validated against the optimizer results before they were assembled into the full system model. In figure 11, sCO_2 flow connections are marked with ‘black’ lines, control system components and connections are marked with ‘green’ lines and mechanical connections are marked with ‘red’ lines.

For comparison with steady state TEOC model, the GT-Suite model was simulated for steady state operation over the ambient temperature range with no gas turbine components connected. For this steady state simulation of GT-Suite transient model, the boundary conditions were exhaust flow rate, exhaust temperature and ambient temperature. Figure 12 gives the comparison plot for sCO_2 net cycle power output. Table 1 gives detailed transient model results for 15 °C ambient temperature for comparison with steady state TEOC results. As can be noted, the agreement is excellent.

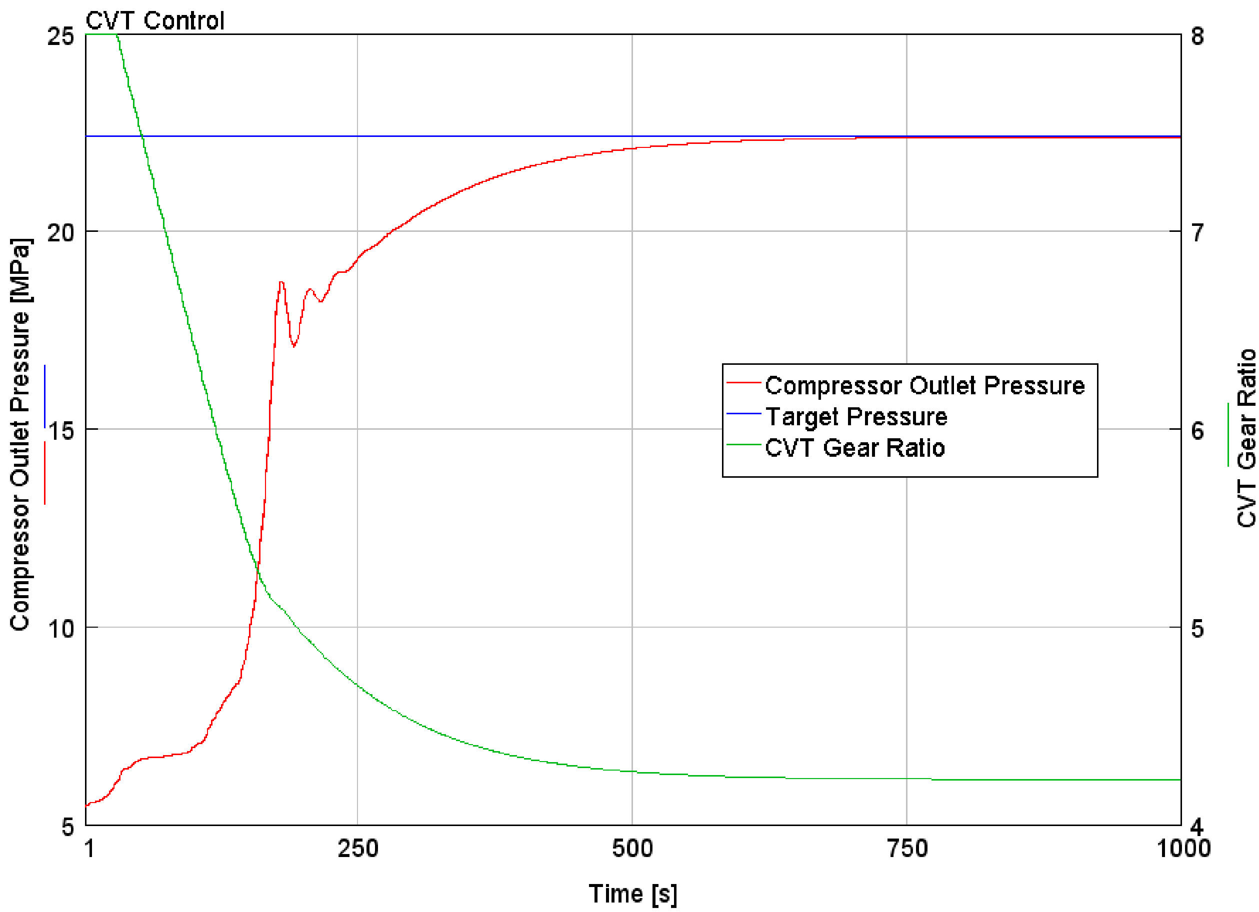

Figure 10: The compressor outlet pressure is maintained at setpoint by varying CVT gear ratio.

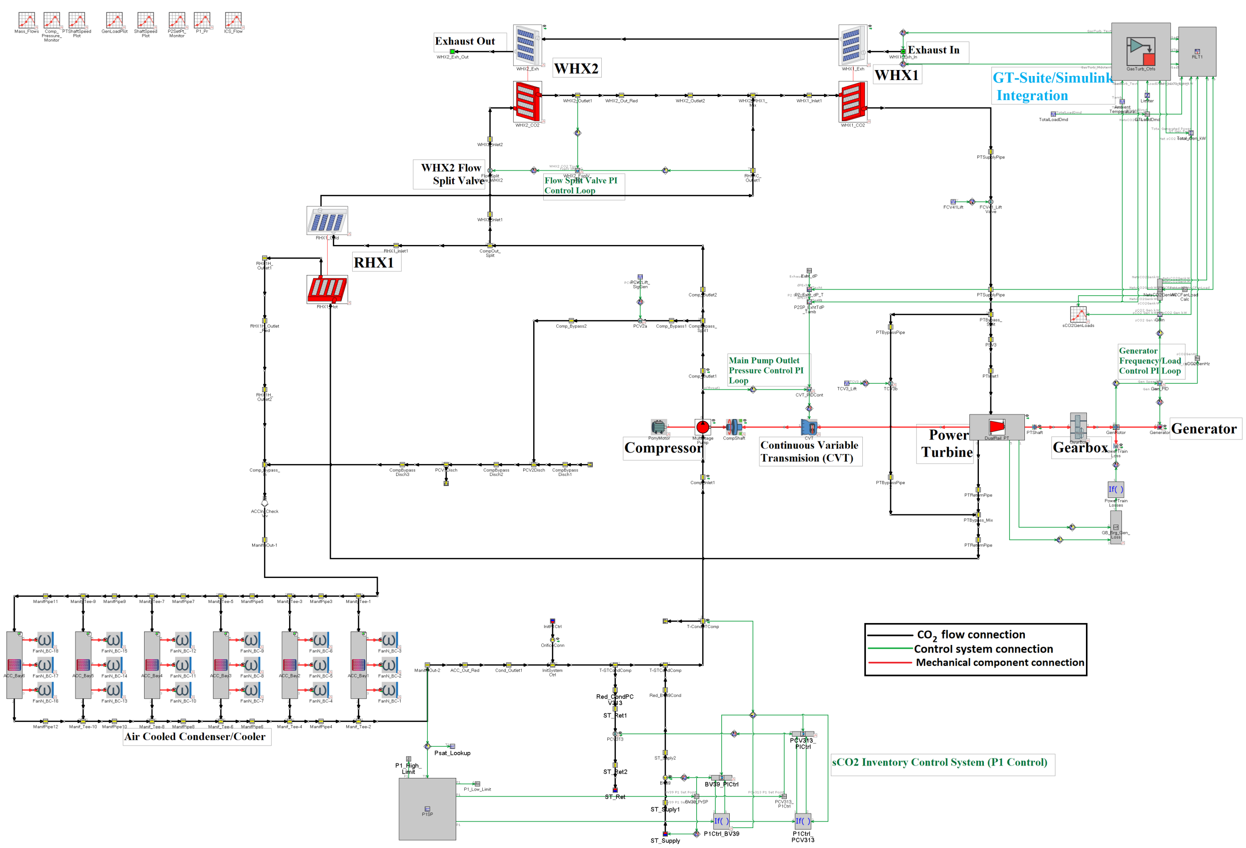

Figure 11: Schematic of sCO_2 power cycle model in GT-SUITE system simulation software platform.

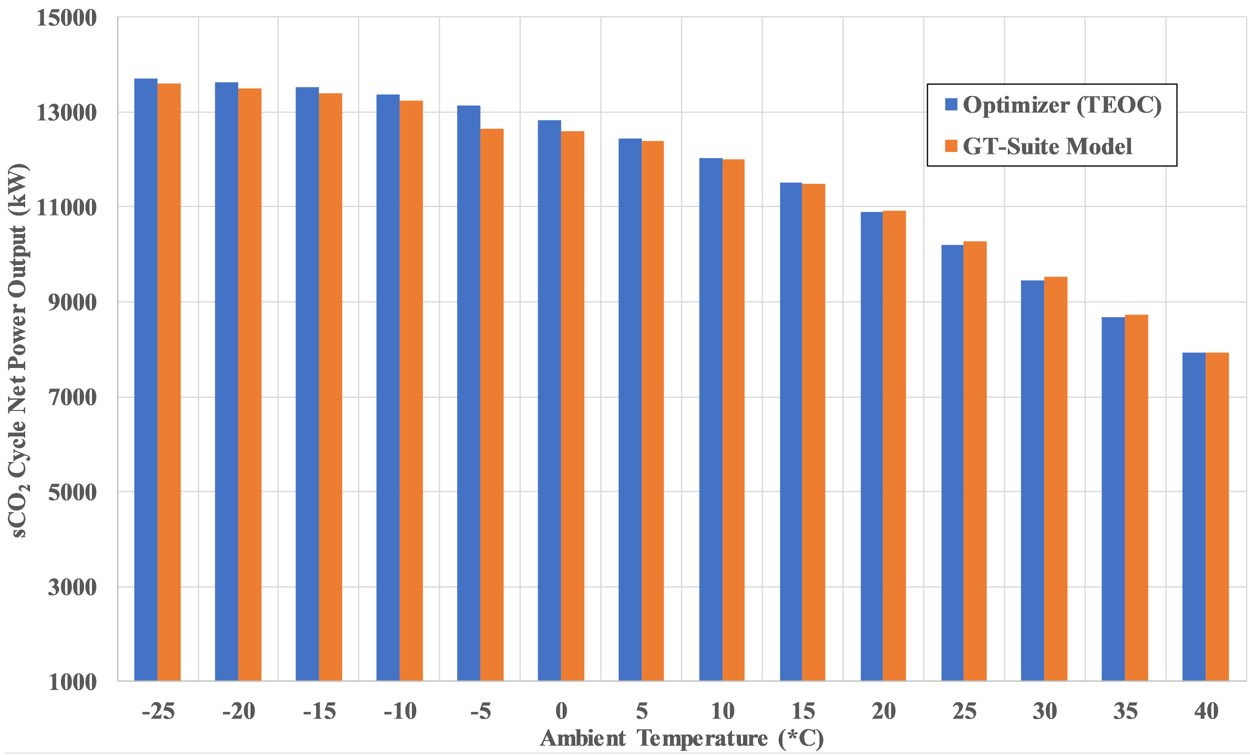

Figure 12: sCO_2 cycle net power output comparison for GT-SUITE model and TEOC model

3 Transient Models Assembled

Echogen has successfully integrated the combined-cycle transient models for SGT-750 with sCO_2 power cycle and also successfully simulated the integrated model using step grid load demand profile. Figure 11 and Figure 13 shows the integration of SGT-750 transient model FMU in Simulink with sCO_2 transient model developed in GT-SUITE. No major issues were noticed in the integration of these transient models. A 5 MWe load demand profile was used as input for combined-cycle comprising of SGT-750 transient and sCO_2 transient models for studying combined system performance and control system response time constants.

In the integrated model, the gas turbine and sCO_2 power cycle interact at two points as shown in 14: first, gas turbine exhaust flow rate and temperature are inputs to sCO_2 power cycle model, and second, distribution of grid load demand signal between SGT-750 generator and sCO_2 cycle generator. For a given combined-cycle load demand, the gas turbine load demand is equal to the total demand minus the sCO_2 cycle power generated. For example, if grid load demand signal is 33 MW and sCO_2 power cycle generator output is 8 MW then the SGT-750 generator receives a 25 MW load demand signal.

In summary for the integrated model has only two inputs: (i) combined-cycle load demand or grid load profile for combined-cycle and (ii) ambient temperature. For the present integrated model simulations the ambient temperature is set at 15 °C.

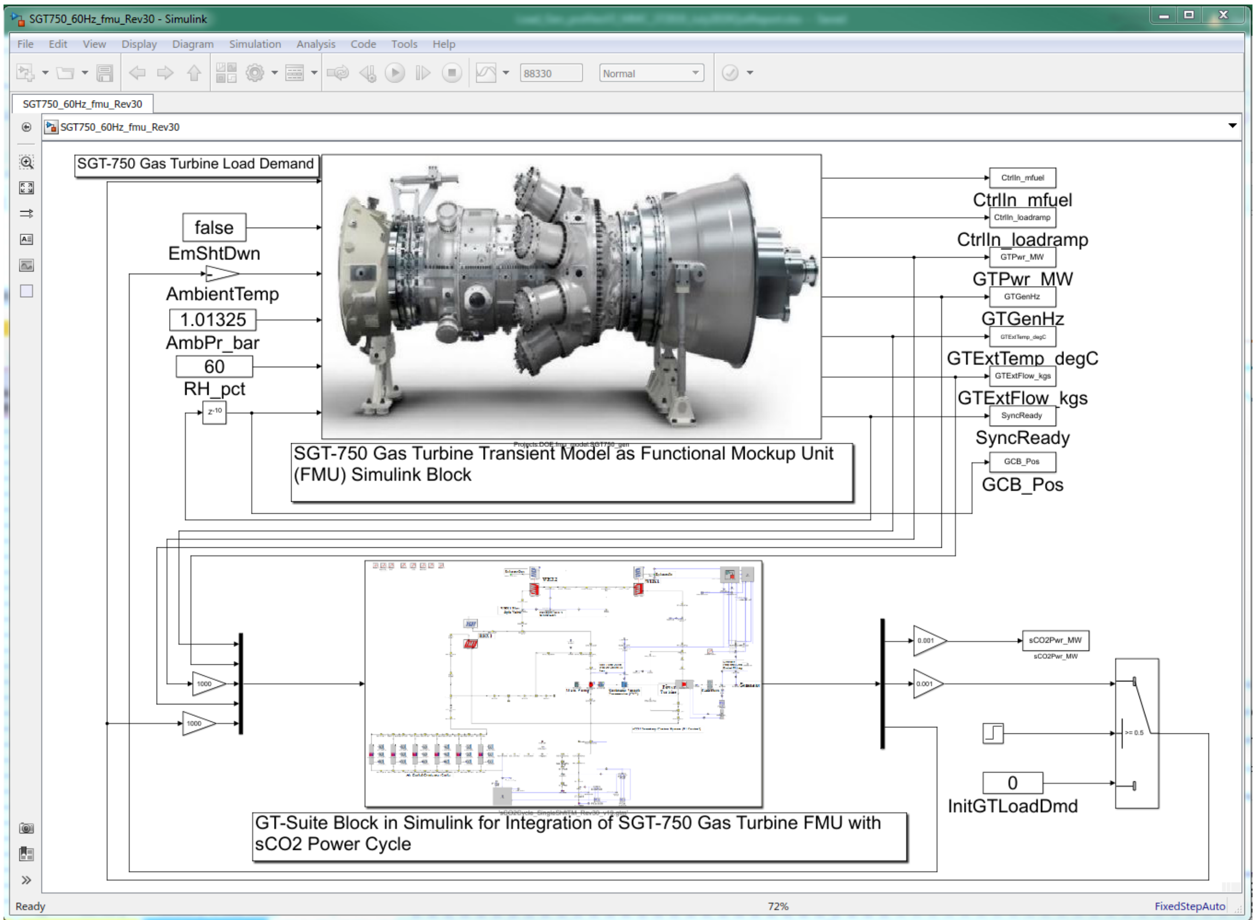

Figure 13: Integration of SGT-750 transient model with sCO_2 transient model in Simulink.

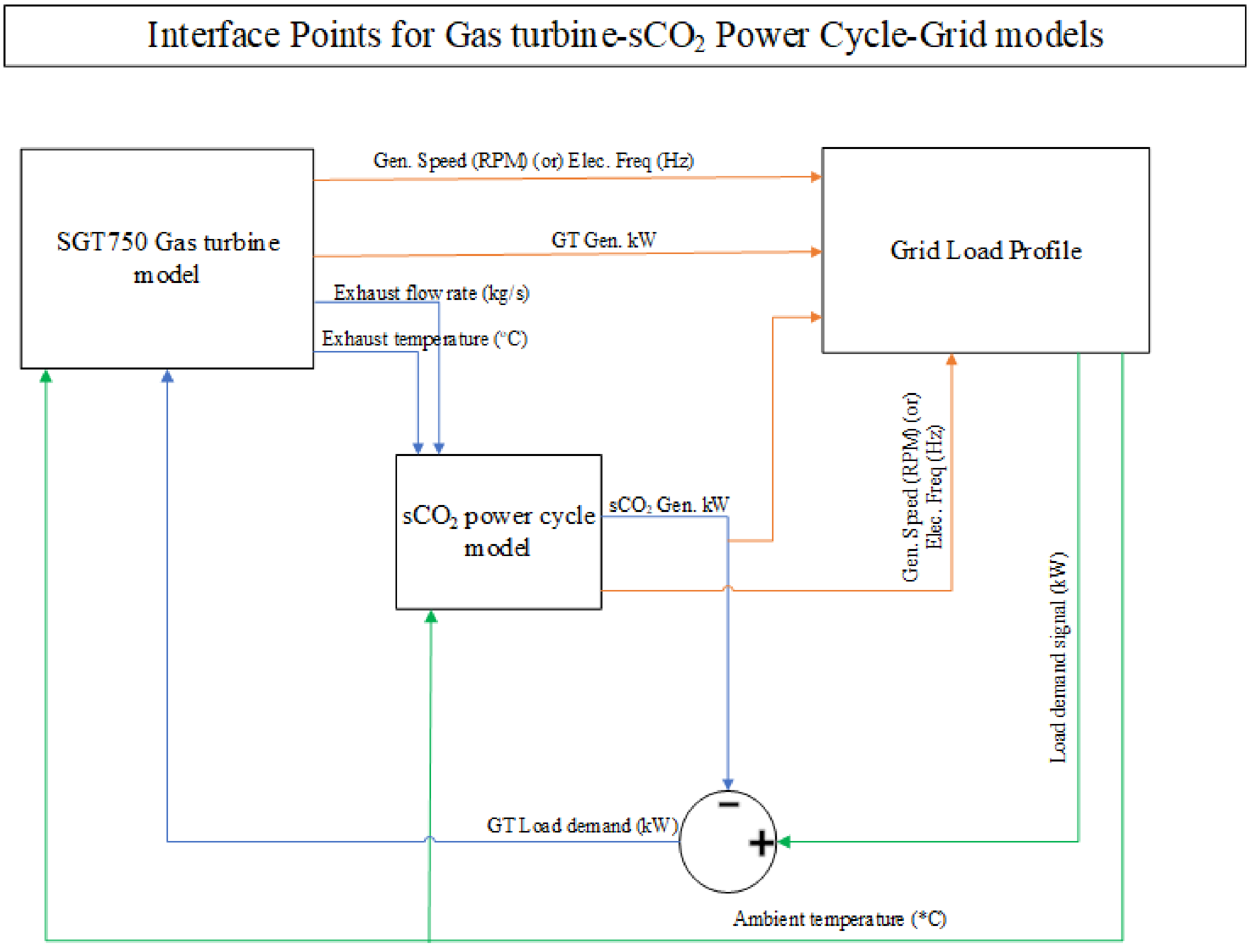

Figure 14: Interface points for SGT-750 transient model and sCO_2 transient model.

4 Results and Discussion

The gas turbine/sCO_2 cycle integrated transient model was simulated using a simple load step response signal for studying the overall system performance and response times. For this, as shown in figure 15, the grid load demand was increased (positive-step) from 35MW to 40MW at 20000s and maintained at 40MW for next 20000s at which point a negative-step load of 5MW was applied to bring back the load to 35MW for rest of the simulation duration.

Figure 16 to figure 22 give the sCO_2 cycle performance results from this run, where '(a)' and '(b)' represents simulation results for positive-step and negative-step respectively. For a step change in grid load demand, the gas turbine response was much faster (figure 16) compared to sCO_2 cycle, which was expected because of the thermal mass effects of waste heat exchangers on sCO_2 cycle. As can be seen the gas turbine generator taking the full step load initially and in about 20 seconds after the step both the cycles again reaching the steady state operation. Figure 17 provides information on variation in gas turbine exhaust flow rate and temperature which are inputs to sCO_2 power cycle model.

In the sCO_2 power cycle operation, compressor inlet pressure (system low pressure) was achieved using a "dead-band" control loop (figure 18) in which the system low pressure is maintained between ± 20 psi from setpoint value and not exactly at setpoint. For example if the low pressure setpoint is 975 psi and the current system pressure is between 955 psi and 995 psi, the inventory control system will be in "stand-by" mode (i.e. supply and return valves closed). But if the system low pressure falls below 955 psi, the ICS supply valve opens to bring system low pressure above 975 psi and similarly if the system low pressure raises above 995 psi, the ICS return valve opens to withdraw fluid until system low pressure falls below 975 psi. Echogen developed this patented methodology for compressor inlet pressure control to provide stable system response and protect against 2-phase flow at the compressor inlet. For both the step response signals the ICS was in "stand-by" mode as can be inferred from figure 18, the two main reasons for this being (i) the current simulations are run at constant ambient temperature of 15 °C and (ii) due to large ACC volume and thereby CO_2 volume, ACC is acting as an "on-board" storage device which can be inferred from figure 19, where the amount of liquid volume in ACC reduces as sCO_2 inlet temperature increases (for positive-step) and the amount of liquid volume in ACC increases as sCO_2 inlet temperature decreases (for negative-step).

Figure 20 shows the CVT control loop's ability to track the set-point compressor outlet pressure. Figure 21 shows the flow split valve performance and the long duration for the valve to reach steady state operation can be attributed mainly to the thermal mass effects of WHX2 coil, which also affects the recuperator performance (heat transfer rate) as shown in figure 22. In this regard, a feed-forward control loop on FSV is being proposed for future improvements of the sCO_2 cycle control system, which may help in achieving faster steady-state and also optimum operation of the power cycle.

To conclude, the successful preliminary integration study of gas turbine and sCO_2 power cycle transient models have paved way for further studies which may include (i) implementation of feed-forward control loops in sCO_2 power system to achieve faster steady-state operation and optimal cycle performance (ii) improving control system strategies using supervisory controls and model predictive controls such that the control system tracks the optimal combined system power output (iii) control system development in industrial control platforms (such as Rockwell Automation, Siemens Controls etc.) for Software-in-Loop (SiL) and later Hardware-in-Loop (HiL) studies which will be useful for power plant operator training.

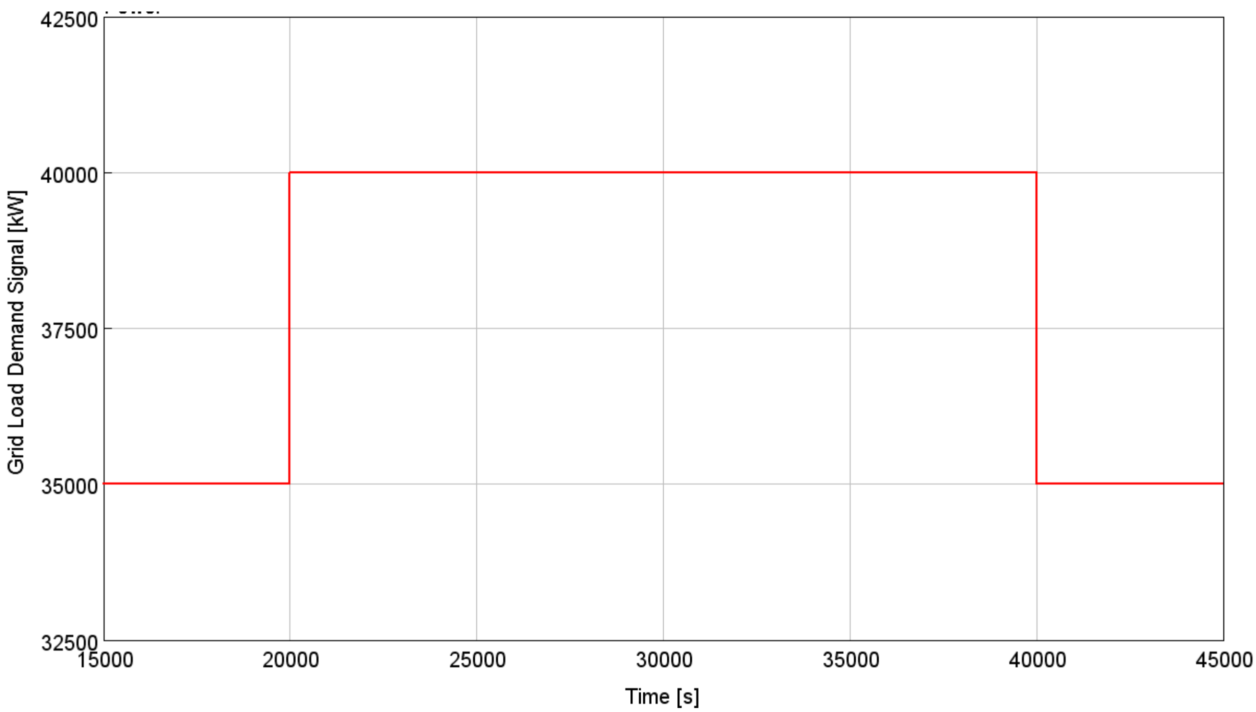

Figure 15: 5MW positive-step (@20000s) and 5MW negative-step (at 40000s) grid load demand signal used for integrated transient model simulation study

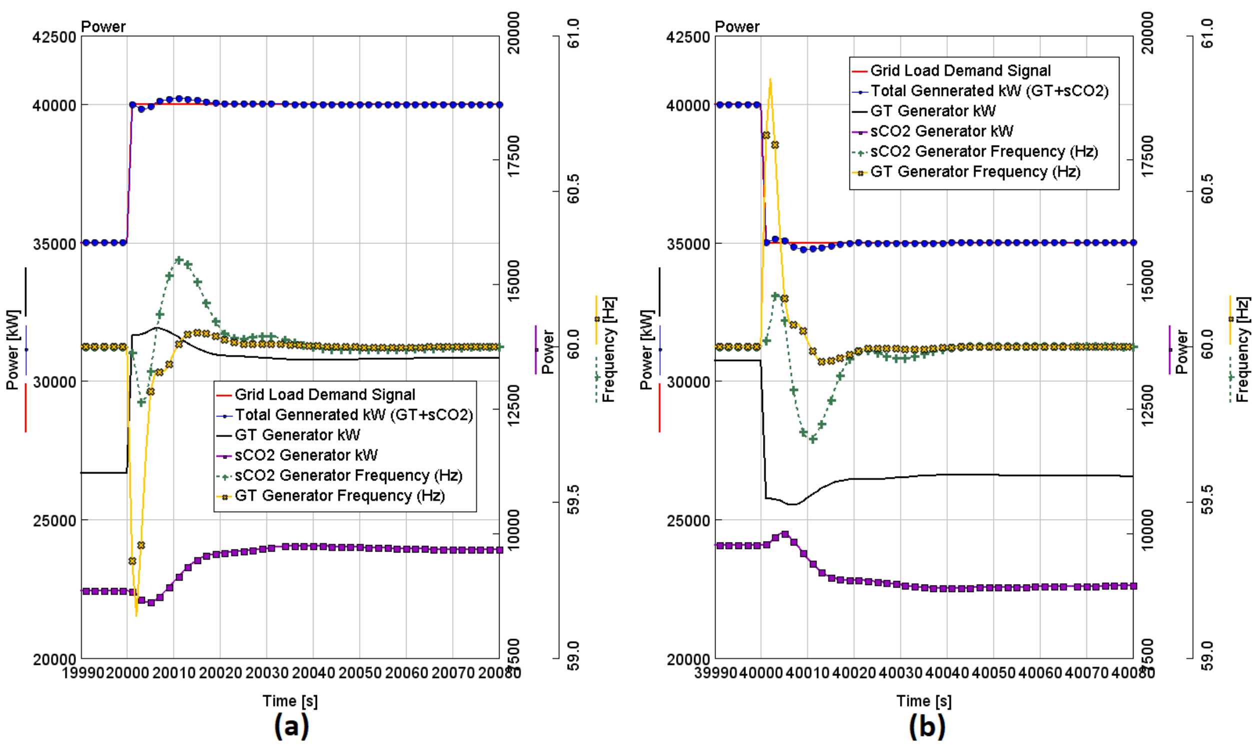

Figure 16: Gas turbine and sCO_2 power cycle generator response to (a) positive-step change and (b) negative-step change in grid load demand

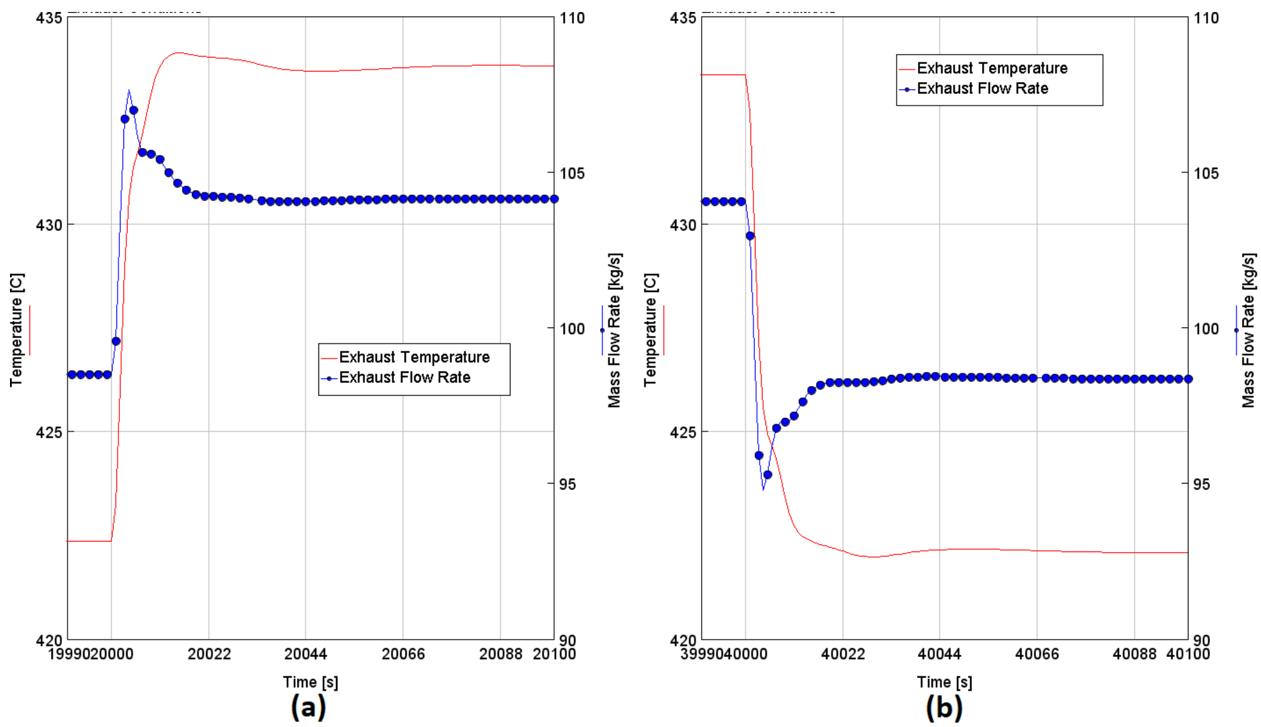

Figure 17: Gas turbine exhaust flow rate and temperature variation to (a) positive-step change and (b) negative-step change in grid load demand

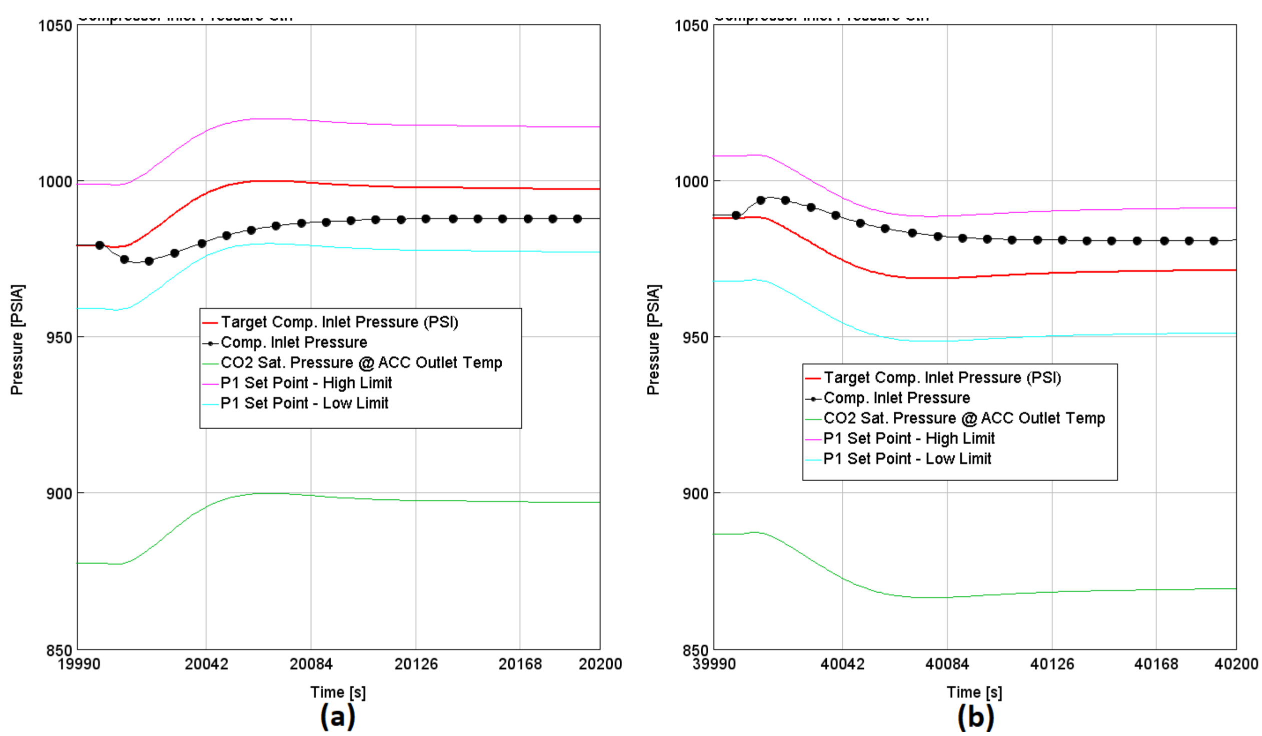

Figure 18: The ability of sCO_2 power cycle control system to maintain compressor inlet pressure for a (a) positive-step change and (b) negative-step change in grid load demand

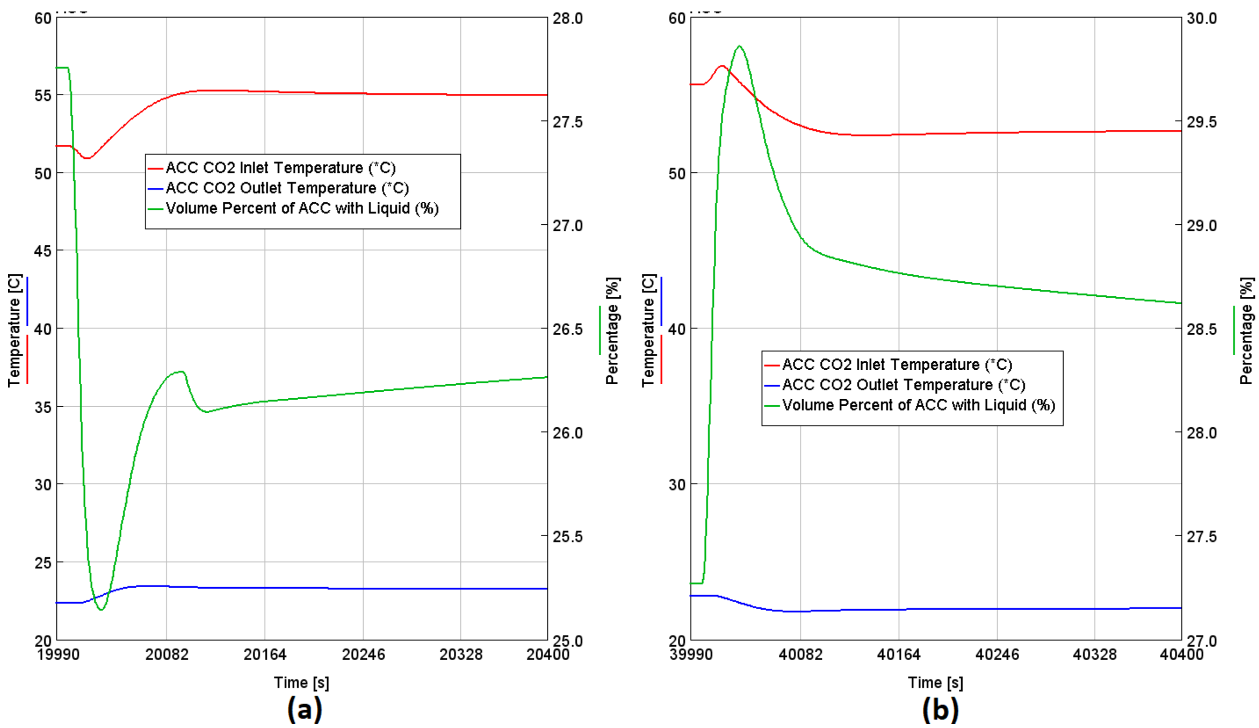

Figure 19: Air cooled condenser performance for a (a) positive-step change and (b) negative-step change in grid load demand

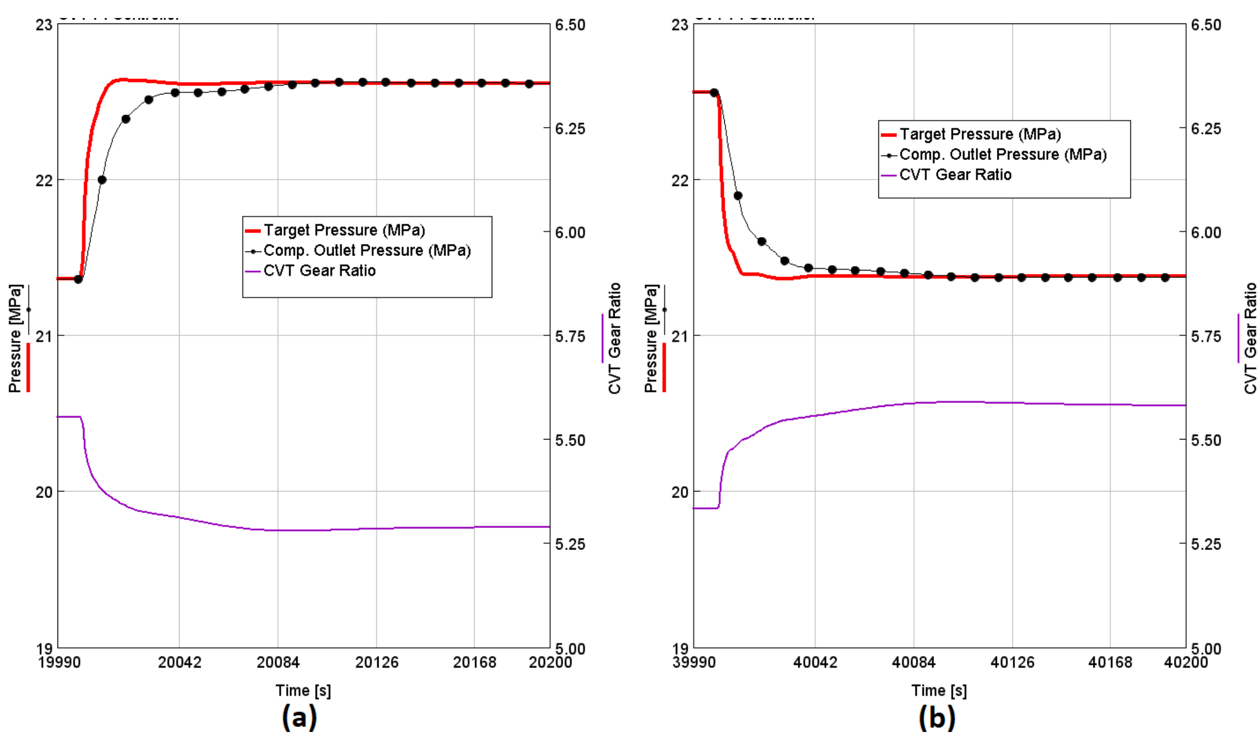

Figure 20: sCO_2 power cycle compressor outlet pressure control using CVT gear ratio for a (a) positive-step change and (b) negative-step change in grid load demand

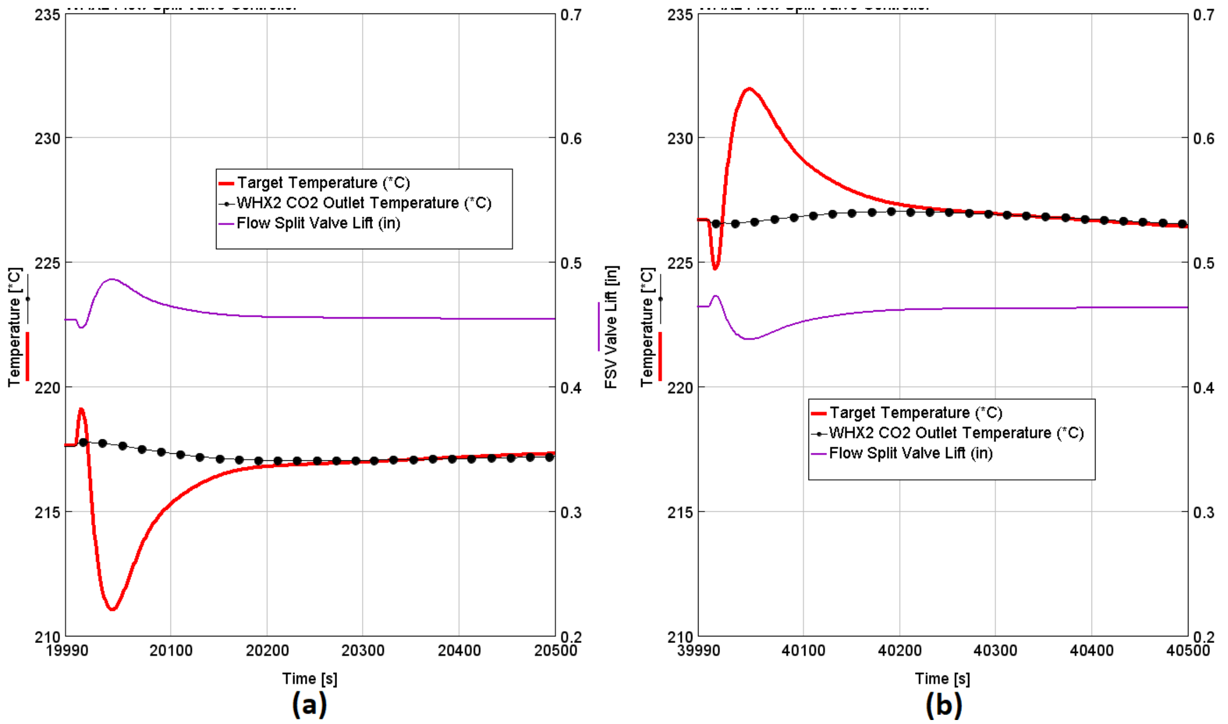

Figure 21: sCO_2 cycle WHX2 outlet temperature control using flow split valve for a (a) positive-step change and (b) negative-step change in grid load demand

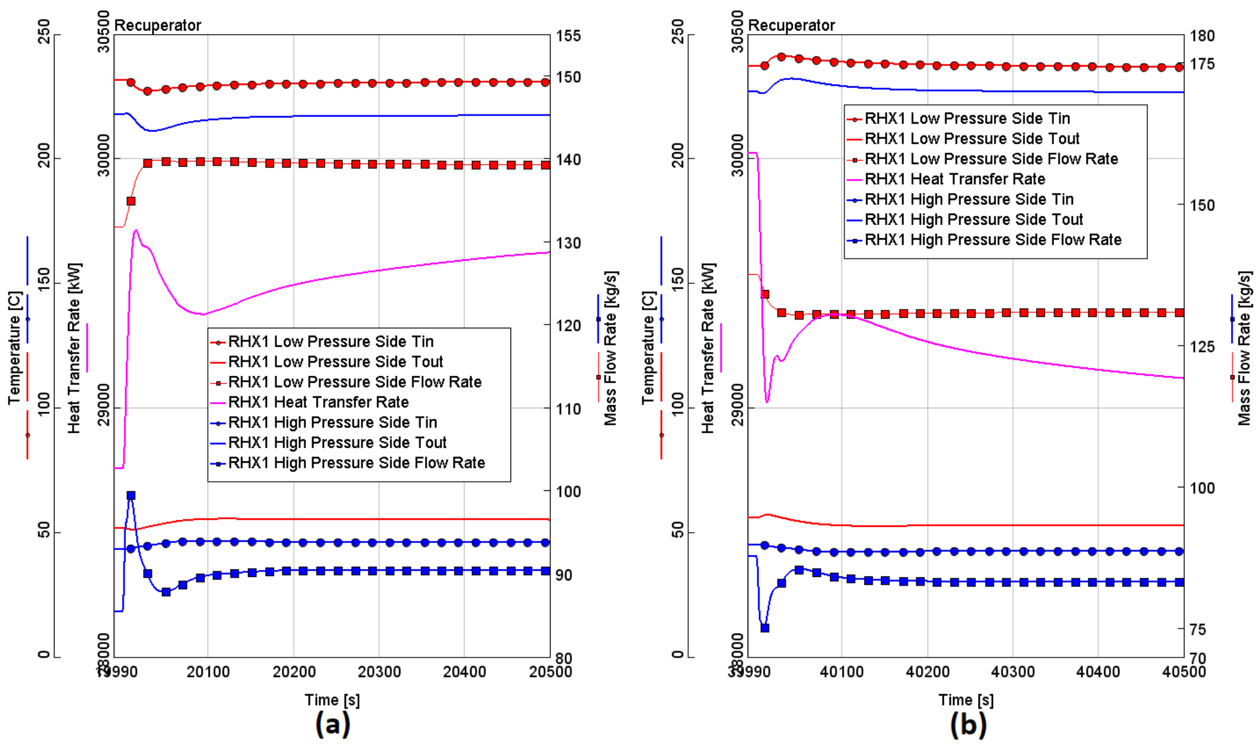

Figure 22: sCO_2 cycle recuperator (RHX1) performance for a (a) positive-step change and (b) negative-step change in grid load demand

Acknowledgments

- This material is based upon work supported by the Department of Energy under Award Number(s) DE-FE0031621.
- Authors would also acknowledge Siemens Finspång (Sweden) for providing SGT-750 gas turbine transient model.

References

[1] Persichilli, M., Held, T. J., Hostler, S., and Zdankiewicz, E., 2011. "Transforming waste heat to power through development of a CO_2-based power cycle". In Proceedings of the 16^{th} International Symposium for Compressor Users-Manufacturers, Echogen Power Systems, p. 9.

[2] Persichilli, M., Kacludis, A., Zdankiewicz, E., and Held, T. J., 2012. "Supercritical CO_2 power cycle developments and commercialization: Why sCO_2 can displace steam". In Proceedings of the Power-Gen India & Central Asia, Echogen Power Systems, p. 15.

[3] Held, T. J., Miller, J., and Buckmaster, D., 2016. "A comparative study of heat rejection systems for sCO_2 power cycles". In Proceedings of the 5^{th} International Supercritical CO_2 Power Cycles Symposium, Echogen Power Systems.

[4] Dostal, V., Driscoll, M., and Hejzlar, P., 2004. A supercrical carbon dioxide cycle for next generation nuclear reactors. Report MIT-ANP-TR-100, MIT Center for Advanced Nuclear Energy Systems, Cambridge, MA, March.

[5] Mendez, C. M., and Rochau, G., 2018. sCO_2 brayton cycle: Roadmap to sCO_2 power cycles ne commercial applications. Technical report SAND2018-6187, Sandia National Laboratories, Albuquerque, NM, June.

[6] Hexemer, M. J., Hoang, H. T., Rahner, K. D., Siebert, B. W., and Wahl, G. D., 2009. "Integrated systems test (IST) S-CO_2 brayton loop transient model description and initial results". In Proceedings of Supercritical CO_2 Power Cycles Symposium, Knolls Atomic Power Laboratory.

[7] Seidel, W., 2010. "Model development and annual simulation of the supercritical carbon dioxide brayton cycle for concentrating solar power applications". Ms thesis, University of Wisconsin-Madison, Madison, WI.

[8] Vijaykumar, R., Bauer, M., Lausten, M., and Shultz, A. M., 2016. "Optimizing the supercritical CO_2 brayton cycle for concentrating solar power application". In Proceedings of the 6^{th} International Supercritical CO_2 Power Cycles Symposium, US Department of Energy.

[9] Turchi, C. S., Ma, Z., Neises, T. W., and Wagner, M. J., 2013. "Thermodynamic study of advanced supercritical carbon dioxide power cycles for concentrating solar power systems". *Journal of Solar Energy Engineering,* **135**(4), June, p. 7. Paper Number: SOL-12-1230.

[10] Walnum, H. T., Nekså, P., Nord, L. O., and Andresen, T., 2013. "Modelling and simulation of CO_2 (carbon dioxide) bottoming cycles for offshore oil and gas installations at design and off-design conditions". *Energy,* **59**(4), September, pp. 513–520.

[11] Held, T. J., 2015. "Supercritical CO_2 cycles for gas turbine combined cycle power plants". In Proceedings of Power-Gen International, Echogen Power Systems, p. 20.

[12] Allam, R. J., Fetvedt, J. E., Forrest, B. A., and Freed, D. A., 2014. "The oxy-fuel, supercritical CO_2 allam cycle: New cycle developments to produce even lower-cost electricity from fossil fuels without atmospheric emissions". In Proceedings of the ASME Turbo Expo: Power for Land, Sea, and Air, Vol. 3B: Oil and Gas Applications; Organic Rankine Cycle Power Systems; Supercritical CO_2 Power Cycles; Wind Energy.

[13] Combs, O. V., 1977. "An investigation of the supercritical CO_2 cycle (feher cycle) for shipboard application". Ms thesis, Massachusetts Institute of Technology, Cambridge, MA, May.

[14] Wright, S. A., Radel, R. F., Vernon, M. E., Rochau, G. E., and Pickard, P. S., 2010. Operation and analysis of a supercritical CO_2 brayton cycle. Technical report SAND2010-0171, Sandia National Laboratories, Albuquerque, NM, September.

[15] Held, T. J., 2014. "Initial test results of a megawatt-class supercritical CO_2 heat engine". In Proceedings of the 4^{th} International Supercritical CO_2 Power Cycles Symposium, Echogen Power Systems.

[16] Avadhanula, V. K., and Held, T. J., 2017. "Transient modeling of supercritical CO_2 power cycle and comparison with test data". In Proceedings of the ASME Turbo Expo: Power for Land, Sea, and Air, Vol. 9: Oil and Gas Applications; Organic Rankine Cycle Power Systems; Supercritical CO_2 Power Cycles; Wind Energy, Echogen Power Systems, p. 15.

[17] Marion, J., 2018. 10 mwe supercritical carbon dioxide (sCO_2) pilot power plant, December. [Accessed on September 16, 2019].

[18] Fayish, P., 2018. Draft environmental assessment for the supercritical carbon dioxide pilot plant test facility. Environmental Assessment Report DOE/EA-2071D, Department of Energy (NETL), San Antonio, TX, March.

[19] Miller, J. D., Mallinak, J., and Held, T. J., 2021. Supercritical carbon dioxide primary power large-scale pilot plant. https://www.osti.gov/biblio/1817332.

[20] FMI Standard, 2015. Functional mock-up interface (fmi 2.0). https://fmi-standard.org.

[21] GT-SUITE, v2019. Gt-suite overview. [Accessed on September 16, 2019].

[22] Lemmon, E. W., Bell, I. H., Huber, M. L., and McLinden, M. O., 2013. Nist standard reference database 23: Reference fluid thermodynamic and transport properties-refprop, version 9.1, national institute of standards and technology.

[23] Avadhanula, V. K., Magyar, L. R., and Held, T. J., 2018. "Printed circuit heat exchanger and finned-tube heat exchanger modeling for a supercritical CO_2 power cycle". In Proceedings of the 6^{th} International Supercritical CO_2 Power Cycles Symposium, Echogen Power Systems.

[24] Pierres, R. L., Southall, D., and Osborne, S., 2011. "Impact of mechanical design issues on printed circuit heat exchangers". In Proceedings of Supercritical CO_2 Power Cycles Symposium, Heatric Division of Meggitt (UK) Ltd.

[25] Dobson, M. K., and Chato, J. C., 1998. "Condensation in smooth horizontal tubes". *ASME Journal of Heat Transfer,* **120**(1), February, pp. 193–213.

[26] Friedel, L., 1979. "Improved friction pressure drop correlation for horizontal and vertical two-phase pipe flow". In Proceedings of European Two-phase Flow Group Meeting, no. Paper number: 2.

[27] Sulzer Pumps. Sulzer pumps catalog. https://www.sulzer.com/en/products/pumps/pumps-by-type. [Accessed on August 15, 2019].